Unsteady natural convection in micropolar nanofluids

KAZIMIERZ RUP[*]
KONRAD NERING

Cracow University of Technology, Faculty of Mechanical Engineering,
Jana Pawła II 37, 31-864 Kraków, Poland

Abstract This paper presents the analysis of momentum, angular momentum and heat transfer during unsteady natural convection in micropolar nanofluids. Selected nanofluids treated as single phase fluids contain small particles with diameter size 10–38.4 nm. In particular three water-based nanofluids were analyzed. Volume fraction of these solutions was 6%. The first of the analyzed nanofluids contained TiO_2 nanoparticles, the second one contained Al_2O_3 nanoparticles, and the third one the Cu nanoparticles.

Keywords: Micropolar fluid; Nanofluid; Heat transfer enhancement

Nomenclature

a	–	fluid thermal diffusivity, m^2/s
c	–	specific heat at constant pressure of the nanofluid
d_p	–	diameter of the nanoparticle, nm
E	–	heat transfer enhancement
Gr_x	–	local Grashof number
g	–	gravitational acceleration, m/s^2
j	–	microinertia density, m^2
k_b	–	Boltzmann constant
M	–	molecular weight of the base fluid; total number of spatial steps in x directions
N	–	microrotation component normal to xy plane, 1/s; total number of spatial steps in y directions

[*]Corresponding Author. E-mail: krup@pk.edu.pl

N_A	–	Avogadro number
n	–	microrotation parameter
Nu_x	–	Nusselt number
P, Δ	–	micropolar fluid parameters
Pr	–	Prandtl number
q_0	–	constant heat flux through the vertical plate
Re	–	Reynolds number
t	–	temperature of fluid, K
T	–	dimensionless temperature
T_w	–	dimensionless wall temperature
T_{fr}	–	freezing point of the base fluid
u, v	–	x and y components of the velocity field, m/s
U, V	–	dimensionless components of the velocity field,
x, y	–	the coordinates of reference system, m
X, Y	–	dimensionless coordinates

Greek symbols

δ	–	hydrodynamic boundary layer thickness
δ_t	–	thermal boundary layer thickness
γ	–	spin gradient viscosity, N s
κ	–	rotational viscosity coefficient, Pa s
λ	–	thermal conductivity, W/(m K)
μ	–	dynamic viscosity, Pa s
ρ	–	density, kg/m^3
$\rho\beta$	–	coefficient of thermal expansion
ρc	–	heat capacity at constant pressure
ϕ	–	nanoparticle volume fraction
σ	–	relative change of temperature
τ	–	time, s
τ_w	–	shear stress of a vertical surface, Pa
▬	–	overbar denotes dimensionless variables

Subscripts and superscripts

i, j	–	grid locations in x, y directions
f	–	properties of base fluid
s	–	properties of solid nanoparticles
∞	–	conditions far away from the wall

1   Introduction

Conventional fluids, such as water, oil, alcohol, glycol ethylene, widely used in heat exchange devices, have relatively low thermal conductivity coefficient. Recently, a new generation of heat carriers known as nanofluids has been developed [1–4]. These types of fluids consist of conventional fluid and nanoparticles with diameter of particle ranging from 10 to 100 nm mixed uniformly with the fluid. Generally, they contain particles of substances

such as Al_2O_3, TiO_2, CuO and Cu [1,4]. The discussed nanofluids are characterized by increased effective thermal conductivity and dynamic viscosity. During experimental studies nanofluids behave like a single phase Newtonian fluid in convectional heat exchange process [2–5]. Recently in [4,5] were presented methods based on a large number of experimental data, used to determine thermophysical parameters of nanofluids. These correlations provide theoretical and practical analysis of heat exchange due to natural convection. Paper [1] analyzes the process of steady natural convection in the nanofluid in the vicinity of a vertical plate heated by applied constant heat flux. In particular the water suspension of Al_2O_3 and CuO was analyzed. Volume fraction of these suspensions did not exceed 10%. A similar work [2] described the natural convection in water suspension of Al_2O_3 at the same thermodynamic conditions. Another paper [3] describes numerical solution of the equations of conservation of mass, momentum and energy in natural convection process in water suspensions of Al_2O_3 and CuO placed in six different closed areas. Increased heat exchange was observed only in triangle-shaped area. The amount of increase was only 5% compared to water without nanoparticles [3].

Due to miniaturisation of heat exchange devices, micropolar fluids as refrigerant or heating media are also analysed in [6–8]. A useful model of micropolar fluid is a model proposed by Eringen. This model takes into account fluid microrotation [6–8].

The aim of work described in this paper is the analysis of increased heat exchange due to natural convection in water solutions of Al_2O_3, TiO_2 and Cu with properties of micropolar nanofluids in the vicinity of vertical plate heated by heat flux of q_0 that rises suddenly.

2   Estimating properties of nanofluids

The typical approach used to study thermodynamic properties of nanofluids is based on the assumption that nanofluids behave like single phase fluids. There are empirical equations proposed by authors used to determine different features of nanofluids such as thermal conductivity, viscosity, density and thermal expansion [4,5]. It is worth mentioning that all models are applicable only in a specific range of nanofluid parameters.

Several authors are proposing different methods to estimate heat conductivity of the nanofluid. This parameter is the most important one with respect to the heat transfer process [4,5]. Based on a large amount of data

presented in [4] a method of heat conductivity calculation was proposed:

$$\lambda = \lambda_f + 4.4 \, \mathrm{Re}^{0.4} \, \mathrm{Pr}_f^{0.66} \left(\frac{T}{T_{fr}} \right)^{10} \lambda_f \left(\frac{\lambda_s}{\lambda_f} \right)^{0.03} \phi^{0.66} \, . \tag{1}$$

This equation is suggested especially when the nanofluid is based on water and glycol ethylene with Al_2O_3, TiO_2, CuO or Cu nanoparticles. In Eq. (1) the Reynolds number is given by equation

$$\mathrm{Re} = \frac{2\rho_f k_b T}{\pi \mu_f^2 d_p} \tag{2}$$

and the Prandtl number as:

$$\mathrm{Pr} = \frac{\mu c \rho}{\lambda \rho} \, . \tag{3}$$

Equation (3) shows that the Prandtl number increases after adding nanoparticles to base fluid.

Many models enabling determining dynamic viscosity have been developed [5]. For example classical no-slip models such as Einstein or Brinkman models yield:

$$\mu = (1 + 2.5 \, \phi) \, \mu_f \, , \tag{4}$$

$$\mu = \frac{\mu_f}{(1 - \phi)^{2.5}} \, . \tag{5}$$

For water suspension of Al_2O_3 nanoparticles, authors recommend the following relationship [4]:

$$\mu = \left(123 \, \phi^2 + 7.3 \, \phi + 1 \right) \mu_f \, . \tag{6}$$

Recently, using a large number of experimental data from several other authors, an empirical equation to determine dynamic viscosity has been proposed [4]:

$$\mu = \frac{\mu_f}{1 - 34.87 \, (d_p/d_f)^{-0.3} \, \phi^{1.03}} \, . \tag{7}$$

To calculate the equivalent diameter of the base fluid molecule from Eq. (7), an equation proposed in [4] was used:

$$d_f = \frac{6M}{N\pi\rho_{f0}} \, . \tag{8}$$

One of the methods to determine density, heat capacity and thermal expansion coefficient is the conventional approach [4,5]. It can be assumed that nanofluid is a single phase fluid. Thus those parameters can be calculated as in case of mixtures. It is given by

$$\rho = (1 - \phi)\,\rho_f + \phi\rho_s \,, \tag{9}$$

$$\rho c = (1 - \phi)\,(\rho c)_f + \phi\,(\rho c)_s \,, \tag{10}$$

$$\rho \beta = (1 - \phi)\,(\rho \beta)_f + \phi\,(\rho \beta)_s \,. \tag{11}$$

In energy equations, heat capacity and thermal expansion coefficient are always considered with fluid density, thus Eqs. (10) and (11) will be used.

3   Problem formulation

In this paper unsteady laminar heat and momentum exchange in nanofluids in terms of natural convection will be considered. Nanofluid is considered in the vicinity of a vertical plate. The heat flux through the plate rises suddenly to the value of q_0.
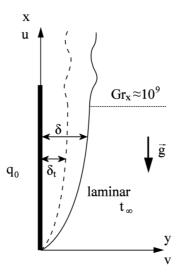

Figure 1: Considered fluid schema, δ – hydrodynamic boundary layer thickness, δ_t – thermal boundary layer thickness.

Problem presented in this work will be solved using the following assumptions:

- Oberbeck-Boussinesq approximation.

- Flow geometry justifies the use of the boundary layer approximation.

- Viscous dissipation and pressure work are neglected.

- Eringen's theory of thermomicrofluid is assumed.

Taking into account the simplification resulting from the boundary layer, the boundary layer theory and fluid density changes according to the Oberbeck-Boussinesq approximation and the following system of equations in dimensionless form can be obtained:

$$\frac{\partial U}{\partial X} + \frac{\partial V}{\partial Y} = 0 \, , \tag{12}$$

$$\frac{\partial U}{\partial \overline{\tau}} + U\frac{\partial U}{\partial X} + V\frac{\partial U}{\partial Y} = (1 + \Delta)\frac{\partial^2 U}{\partial Y^2} + \Delta\frac{\partial \overline{N}}{\partial Y} + T \, , \tag{13}$$

$$\frac{\partial \overline{N}}{\partial \overline{\tau}} + U\frac{\partial \overline{N}}{\partial X} + V\frac{\partial \overline{N}}{\partial Y} = (1 + \frac{\Delta}{2})\frac{\partial^2 \overline{N}}{\partial Y^2} - \Delta(2\overline{N} + \frac{\partial \overline{N}}{\partial Y})P \, , \tag{14}$$

$$\frac{\partial T}{\partial \overline{\tau}} + U\frac{\partial T}{\partial X} + V\frac{\partial T}{\partial Y} = \frac{1}{Pr_\infty}\frac{\partial^2 T}{\partial Y^2} \, . \tag{15}$$

For above equations the initial and boundary conditions will be a dimensionless form:

$$\overline{\tau} < 0 \, , \quad U = V = T = 0 \, , \tag{16}$$

$$\overline{\tau} \geq 0 \, , \quad X = 0 \, , \quad U = V = T = 0 \, , \tag{17}$$

$$Y = 0 \, , \quad U = V = 0 \, , \quad -\frac{\partial T}{\partial Y} = 1 \, , \quad \overline{N} = -n\frac{\partial U}{\partial Y} \, , \tag{18}$$

$$Y \to \infty \quad U = V = T = \overline{N} = 0 \, . \tag{19}$$

Dimensionless parameters from the above equations are defined as:

$$T = \frac{t - t_\infty}{[v_\infty^2(\frac{q_0}{\lambda})^3\frac{1}{g\beta}]^{\frac{1}{4}}} \, , \qquad \overline{\tau} = \frac{\tau}{[(\frac{\lambda}{q_0})\frac{1}{g\beta}]^{\frac{1}{2}}} \, , \tag{20}$$

$$U = \frac{u}{[v_\infty^2\frac{q_0}{\lambda}g\beta]^{\frac{1}{4}}} \, , \qquad V = \frac{v}{[v_\infty^2\frac{q_0}{\lambda}g\beta]^{\frac{1}{4}}} \, , \tag{21}$$

$$X = \frac{x}{[v_\infty^2\frac{\lambda}{q_0}\frac{1}{g\beta}]^{\frac{1}{4}}} \, , \qquad Y = \frac{y}{[v_\infty^2\frac{\lambda}{q_0}\frac{1}{g\beta}]^{\frac{1}{4}}} = \frac{y}{x}(\mathrm{Gr}_x)^{\frac{1}{4}} \, , \tag{22}$$

$$\mathrm{Gr}_x = \frac{g\beta}{v_\infty^2}\frac{q_0}{\lambda}x^4\,, \qquad \overline{N} = N[g\beta\frac{q_0}{\lambda}]^{-\frac{1}{2}}\,, \tag{23}$$

$$\Delta = \frac{\kappa}{v_\infty \rho}\,, \qquad P = \frac{v_\infty}{j}\frac{1}{(\frac{q_0}{\lambda}g\beta)^{\frac{1}{2}}} = \frac{x^2}{j}(\mathrm{Gr}_x)^{-\frac{1}{2}}\,. \tag{24}$$

In Eq. (18) similarly to [2–6] the relation between microrotation component normal to xy-plane and velocity gradient (shear stress) on the plate was assumed. The value of microrotation parameter n from Eq. (18) is between 0 and 1 [7,8]. The value $n = 0$ corresponds to the case of the high density of liquid microparticles that prevents them from performing rotational movements. The value $n = 0.5$ is indicative of weak concentrations and the value $n = 1$ is representative for turbulent boundary layer [7,8].

Parameters occurring in Eq. (24) such as microinertia density, rotational viscosity coefficient and spin gradient viscosity are related to the following equation [6–8]:

$$\gamma = \left(\mu + \frac{\kappa}{2}\right)j\,. \tag{25}$$

The set of partial differential equations (12)–(15) together with initial and boundary conditions (16)–(19) will be solved numerically using the finite difference method [8,9].

4 Problem solution

Equations (12)–(15) will be solved using explicit finite difference scheme. Spatial distribution grid contains $M \times N$ points in the X and Y directions respectively, $\Delta\overline{\tau}$ is the time step. Due to the intensive heat, momentum, angular momentum and mass transfer, only in the direct vicinity of the considered vertical surface, the maximum values of dimensionless coordinates $X = 100$ and $Y = 30$ were assumed [8]. A characteristic feature of the difference equations was to determine the temperature field, the velocity field components and the microrotation component $\overline{N}$ at time $\overline{\tau}_{n+1}$ depending on certain parameters, but determined at time $\overline{\tau}_n$. Convection terms of balance equations comprising time $\overline{\tau}$ derivatives and spatial Y coordinate derivatives were approximated by 'forward' formulas whereas spatial X coordinate derivatives were approximated by "backward" formulas. Diffusion terms were approximated by central differences. Derivatives appearing in the boundary conditions (18) were approximated by higher order difference

formulas taken in the form [9]:

$$\frac{\partial T}{\partial Y_{|ij}} = \frac{1}{6\Delta Y}\big(-11T_{ij} + 18T_{i,j+1} - 9T_{i,j+2} + 2T_{i,j+3}\big) + O[\Delta Y]^3\,, \quad (26)$$

$$-\frac{1}{n}\overline{N_{|i,j}} = \frac{\partial U}{\partial Y_{|ij}} = \frac{1}{12\Delta Y}\big(-25U_{i,j} + 48U_{i,j+1} -$$
$$-36U_{i,j+2} + 16U_{i,j+3} - 3U_{i,j+4}\big) + O[\Delta Y]^4\,. \quad (27)$$

These difference formulas are statically stable and exhibit characteristics of conservation [9].

Before performing basic numerical calculations for the established, non-zero values of parameters Δ and P describing the properties of micropolar fluid, calculation tests were done similarly to [8]. In the process of steady natural convection in a Newtonian fluid, the exact analytical solutions are known [10], and were compared to the corresponding calculation results. On the basis of preliminary calculations, further ones, taking into account the nonzero values of Δ and P parameters, were performed with the following spatial area division: $M \times N = 250 \times 150$, the time step $\Delta\overline{\tau} = 0.002$. Assumed area division is smaller than area division in work [8] and the time step is two times greater. This change of area division and time step needs to be done to obtain greater accuracy of the applied differential forms.

5   Results and discussion

The set of Eqs. (12)–(15) with initial condition (16) and boundary conditions (17)–(19) were integrated for the selected values of parameters Pr, P, Δ and n. Water (W) in temperature of 60 ºC was the base fluid. The Prandtl number of base fluid was 3.00. In the next stage of analysis it was assumed that base fluid has micropolar features with the following parameters: $\Delta = 5.0$, $P = 1.0$ and $n = 0.5$. These parameters were assumed based on literature data and previous own works [7,8].

Main analysis was focused on the effects occurring in nanofluids. In this work, the following homogeneous water solutions of nanoparticles were analysed:

- water solution of Al_2O_3 nanoparticles with mean diameter of 38.4 nm,
- water solution of TiO_2 nanoparticles with mean diameter of 27 nm,

- water solution of Cu nanoparticles with mean diameter of 10 nm.

Nanoparticle volume fraction for the above solutions was $\phi = 6\%$. Parameters describing these solutions for temperature 60 °C calculated using Eqs. (1)–(8) are presented in Tab. 1.

Table 1: Thermophysical parameters of water-based nanofluids in temperature $t_\infty = 60$ °C.

Fluid	Density, ρ [kg/m³]	Dynamic viscosity, μ [kg/(m s)]	Thermal conductivity, λ [W/(m K)]	Heat capacity, ρc_p [J m³/K]	Thermal expansion, $\rho\beta$ [kg/(K m³)]	Prandtl number, Pr	Normalised coordinates X/X_f; Y/Y_f	Normalised parameter Δ/Δ_f	Normalised parameter P/P_f
Water (W)	983.24	4.688×10^{-4}	0.6590	4111221.4	0.4956	3.00	1.000	1.000	1.000
W + TiO$_2$ (27 nm)	1178.05	1.015×10^{-3}	1.0063	4040178.0	0.4681	3.4599	0.631	0.462	2.515
W + Al$_2$O$_3$ (38.4 nm)	1157.05	0.9089×10^{-3}	0.9757	4042640.1	0.4678	3.253	0.668	0.516	2.238
W + Cu (10 nm)	1460.65	1.705×10^{-3}	1.2392	4071062.1	0.4932	3.8347	0.494	0.275	4.102

Figure 2 shows the U velocity component in the X-axis direction for water (Pr = 3.00) and two different nanofluids with Prandtl number Pr = 3.253 and 3.460 at fixed times of the process $\overline{\tau} = 10$, 20, and 80. In order to simplify the analysis the thermophysical parameters values for Δ and P were considered to equal zero. Figure 2 shows three different cases with characteristic value of Grashof number $Gr_x = 10^8$. For the assumed Grashof number, dimensionless coordinate X adopts values from Tab. 1. For nanofluids, this X value equals respectively $X^{TiO2} = 0.631\,X_f$ and $X^{Al2O3} = 0.668\,X_f$. Line marked with circles represents results for water as the base fluid. Lines marked with triangles and squares represent results of velocity component U in nanofluids. Maximum values of velocity component U are lower than corresponding values for water in the entire range of $\overline{\tau}$.

Figure 3 presents temperature profiles in the considered liquids at certain moments of the process, namely $\overline{\tau} = 10$, 20 and 80. Similarly as for the U velocity component, proper values of parameters describing the thermophysical properties of the fluid were assumed. Furthermore temperature profile in fluid with micropolar features ($\Delta = 5.0$ and $P = 1.0$) was pre-
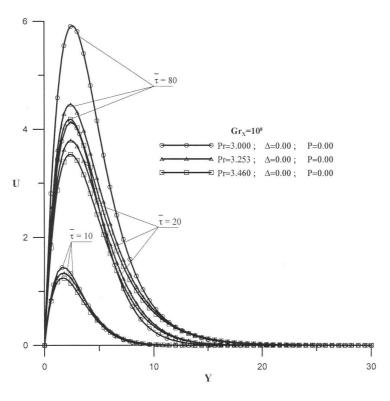
Figure 2: Profiles of the velocity component U at selected moments of the process.

sented only for the time $\overline{\tau} = 80$. This profile, represented by the dashed line, indicates significantly larger temperature values than other fluids. Temperature of the heated plate is the largest for the fluid with micropolar features. Maximal relative increase of temperature of the heated plate for micropolar fluid in the last stage of the process is $\sigma = (T_w - T_w^f)/T_w^f = 0.230$. High temperature of the heated vertical plate indicates significantly smaller intensity of heat interception by the analyzed micropolar fluid than other fluids. Figure 3 shows larger rate of heat interception intensity in the entire range of time in comparison with water. Values of σ parameter for the analyzed nanofluids are: $\sigma_{Cu} = -0.186$; $\sigma_{TiO2} = -0.122$ and $\sigma_{Al2O3} = -0.098$.

On the basis of temperature profile distribution the local Nusselt number Nu_x in the analyzed fluid on heated vertical plate yields

$$\mathrm{Nu}_x = \frac{q_0}{t_w - t_\infty} \frac{x}{\lambda} \ . \tag{28}$$
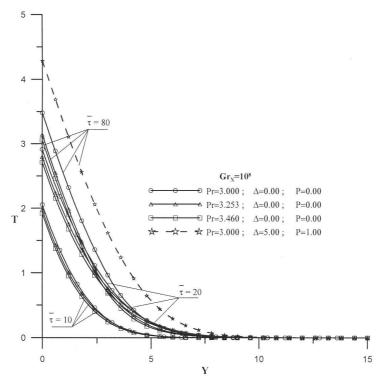
Figure 3: Profiles of the fluid temperature changes.

Using dimensionless Eqs. (20)–(24) with the Nusselt number (28) we obtain

$$\frac{\mathrm{Nu}_x}{\mathrm{Gr}_x^{\frac{1}{5}}} = X^{\frac{1}{5}} \frac{1}{T_w} \ , \tag{29}$$

where

$$T_w = \frac{t_w - t_\infty}{[v_\infty^2 (\frac{q_0}{\lambda})^3 \frac{1}{g\beta}]^{\frac{1}{4}}} \ . \tag{30}$$

The relationship (29) is shown graphically in Fig. 4. For the sake of comparison, Fig. 4 comprises the corresponding curve obtained for pure water. Curves from Fig. 4 represent local Nusselt number with respect to local Grashof number ($\mathrm{Nu}_x/(\mathrm{Gr}_x)^{1/5}$), where the value of $\mathrm{Gr}_x = 10^8$. It is worth mentioning that corresponding lines of the parameter $\mathrm{Nu}_x/(\mathrm{Gr}_x)^{1/5}$ have different dimensionless X coordinate. For pure water, coordinate $X = X_f = 100$ corresponds, due to Eqs. (22) and (23), to the Grashof

number $\mathrm{Gr}_x = 10^8$. For the same Grashof number, the dimensionless coordinate X is $X^{TiO2} = 0.631\, X_f$; $X^{Al2O3} = 0.668\, X_f$ and $X^{Cu} = 0.494\, X_f$, respectively for the considered nanofluids. As indicated in Fig. 4, the intensity of heat exchange in micropolar fluid is significantly lower than in corresponding nanofluids.
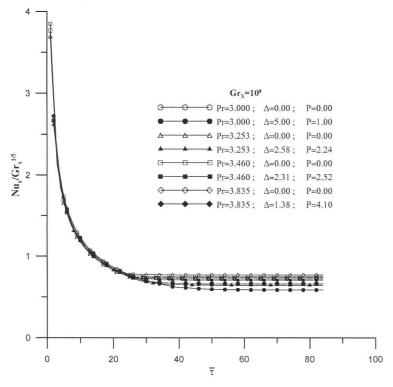

Figure 4: Transient changes of the local Nusselt number.

On the basis of calculated velocity field, a shear stress on a vertical plate was determined. Taking into account constitutive equations for micropolar fluid [1,2]

$$\tau_w = \left[(\mu + \kappa)\frac{\partial u}{\partial y} + \kappa N\right]_{|y=0}. \tag{31}$$

After incorporation of dimensionless Eqs. (21)–(24) into the above one we obtain

$$\overline{\tau}_w = \frac{\tau_w}{\frac{\rho_\infty v_\infty^2}{x^2}5^{2/5}\mathrm{Gr}_x^{3/5}\left(1 + \Delta - n\Delta\right)} = \frac{1}{(5X)^{2/5}}\frac{\partial U}{\partial Y}_{|y=0}. \tag{32}$$

In order to make a comparative analysis, Tab. 2 summarizes the Nusselt number values determined according to the formula (29) and the dimensionless shear stress in accordance with formula (32), obtained from the numerical calculations performed for the variable parameters Δ, P, Pr and constant parameter n ($n = 0.5$). The summarized results relate to the steady state with the Grashof number 10^8, which is reached for the nanofluid when dimensionless coordinate X is lower than X coordinate for pure water ($X_f = 100$). This coordinate is measured along the vertical plate. Exact values of the quotient X/X_f and Y/Y_f (Tab. 1) were determined according to relationships (1), (7), (9), (10), and (22), taking into account respective values of thermophysical parameters of pure water and considered nanofluids. In Tab. 2 values with asterisk (*) were taken from [10]. Result from [10] was compared with the exact analytical solution of conservation equations for the Newtonian fluid.

Table 2: A comparison of results.

Pr	Δ	P	$\mathrm{Nu}_x/\mathrm{Gr}_x^{\frac{1}{5}}$	$\overline{\tau}_w$
3.0 W	0.0	0.0	0.7108*	0.5054*
	0.0	0.0	0.72091	0.47181
	5.0	1.0	0.58602	0.22234
3.253 W + Al$_2$O$_3$ (38.4 nm)	0.0	0.0	0.7252*	0.4918*
	0.0	0.0	0.73755	0.45634
	2.580	2.238	0.64371	0.27699
3.460 W + TiO$_2$ (27 nm)	0.0	0.0	0.7362*	0.4806*
	0.0	0.0	0.7492	0.44595
	2.310	2.515	0.66001	0.28093
3.8347 W + Cu (10 nm)	0.0	0.0	0.75493*	0.46020*
	0.0	0.0	0.76869	0.42822
	1.375	4.102	0.70548	0.31111

* values taken from [10]

Figure 5 presents the dimensionless shear stress according to Eq. (32) during natural convection. Presented curves are characteristic for the indicated Prandtl number, parameters Δ, P, $n = 0.5$ and constant value of Grashof number equal to 10^8. Before time $\overline{\tau} = 30$ the dimensionless shear stress grows rapidly, and after time $\overline{\tau} = 30$ this shear stress on heated vertical plate is determined by a constant value. This increase of the shear stress

value is characteristic for the initial period of natural convection wherein conductive heat exchange is significant. Due to the increase of Δ and P values the dimensionless shear stress is decreasing similarly to the parameter $\mathrm{Nu}_x/(\mathrm{Gr}_x)^{1/5}$, showed in Fig. 4.
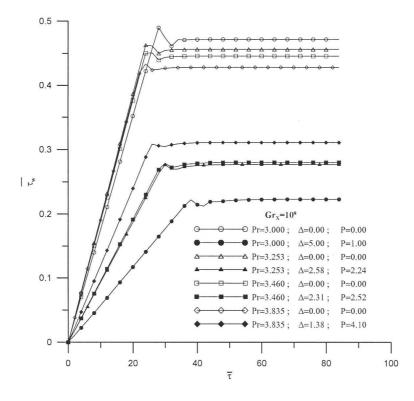

Figure 5: Transient changes of dimensionless shear stress on vertical plate.

Heat transfer enhancement during natural convection in the considered nanofluids is represented by the following equation:

$$E = \frac{\dfrac{\mathrm{Nu}_x}{\mathrm{Gr}_x^{1/5}}}{\left.\dfrac{\mathrm{Nu}_x}{\mathrm{Gr}_x^{1/5}}\right|_f} - 1 \ . \tag{33}$$

Table 3 presents values of E parameters calculated with relationship (33) for the considered nanofluid in the stationary case. In calculating of these values the corresponding results from Tab. 2 were used. Maximum value of

E parameter is found for the nanofluid with Cu nanoparticles with mean diameter of 10 nm.

Table 3: Obtained values of the E parameter with respect to Eq. (33).

Fluid	Δ	P	$\mathrm{Nu}_x/\mathrm{Gr}_x^{\frac{1}{5}}$	E [%]
W	0.0	0.0	0.72091_f	–
W + Al$_2$O$_3$ (38.4 nm)	0.0	0.0	0.73755	2.31
W + TiO$_2$(27 nm)	0.0	0.0	0.7492	3.92
W + Cu (10 nm)	0.0	0.0	0.76869	6.70
W (micropolar)	5.0	1.0	0.58602_f	–
W + Al$_2$O$_3$(38.4 nm)	2.580	2.238	0.64371	9.8
W + TiO$_2$(27 nm)	2.310	2.515	0.66001	12.6
W + Cu (10 nm)	1.375	4.102	0.70548	20.4

6   Concluding remarks and conclusion

In this paper, a process of heat and momentum exchange during natural convection in nanofluids with micropolar properties was analyzed. To describe the analyzed phenomena of exchange, equations of hydrodynamic and thermal boundary layer were used. It is worth noting that coupled system of differential equations describing the analyzed exchange process also includes, in accordance with the boundary layer theory, a simplified equation for the $\overline{N}$ microrotation component, arising from the angular momentum principle. In order to solve this problem the method of finite difference was applied. Obtained results were presented in graphs and in tables.

Parameter E describing the heat transfer enhancement between heated plate and the nanofluid showed in Tab. 3, appears to have a maximum value equal 6.7% which was obtained for the nanofluid with Cu nanoparticles with the mean diameter of 10 nm and parameters Δ and P equal to zero. For the same fluid, relative decrease of temperature of the heated vertical plate was $\sigma_{Cu} = 18.6\%$ at the end of analyzed process in time $\overline{\tau} = 80$. For nanofluids with Al$_2$O$_3$ nanoparticles with mean diameter 38.4 nm, relative decrease of temperature of the heated vertical plate was only 9.6%.

Micropolar fluids are the fluids with nonzero values of Δ and P parameters. These fluids are characterized by different behaviour during natural

convection. Calculation results obtained in this work for fluids with parameters $\Delta = 5.0$ and $P = 1.0$ show that the dimensionless shear stress for micropolar fluids on a heated plate has lower values than the corresponding values for Newtonian fluid during the entire process of heating. Maximal relative change of τ_w is equal to 52.7% ($\Delta = 5.0$, $P = 1.0$) and maximal relative change of $\mathrm{Nu}_x/(\mathrm{Gr}_x)^{1/5}$ value for micropolar fluid with respect to Newtonian fluid equals 18.4%.

Significantly higher value of temperature of the heated plate can be found after time $\overline{\tau} = 10$ in the vicinity of micropolar fluid which indicates lower intensity of heat interception by the analyzed micropolar fluid compared to the Newtonian fluid. The highest changes of microrotation component $\overline{N}$ are observed before time $\overline{\tau} = 10$ at the beginning of the process.

References

[1] POPA C., FOHANNO S., NGUYEN C.T., POLIDORI G.: *On heat transfer in external natural convection flows using two nanofluids.* Int. J. Therm. Sci. **49**(2010), 901–908.

[2] POLIDORI G., FOHANNO S., NGUYEN C. T.: *A note on heat transfer modeling of Newtonian nanofluids in laminar free convection.* Int. J. Therm. Sci. **46**(2007), 739–744.

[3] ABUALI O., AHMADI G.: *Computer simulations of natural convection of single phase nanofluids in simple enclosures: A critical review.* Appl. Therm. Eng. **36**(2012), 1–13.

[4] CORICONE M.: *Empirical correlating equations for predicting the effective thermal conuctivity and dynamic viscosity of nanofluids.* Energy Convers. Manage. **52**(2011), 789–793.

[5] KAKAÇ S., PRAMUANJAROENKIJ A.: *Review of convective heat transfer enhancement with nanofluids.* Int. J. Heat Mass Tran. **52**(2009), 3187–3196.

[6] ERINGEN A.C.: *Theory of micropolar fluids.* J. Math. Mech. **16**(1966), 1–18.

[7] MOHAMMEDAN A.A., GORLA R.S.R.: *Heat transfer in a micropolar fluid over a stretching sheet with viscous dissipation and internal heat generation.* Int. J. Numer. Method H. **11**(2001), 1, 50–58.

[8] RUP K., DRÓŻDŻ A.: *The effect of reduced heat transfer in micropolar fluid in natural convection.* Arch. Thermodyn. **34**(2013), 3, 45–59.

[9] TANNEHILL J.C., ANDERSON A.D., PLETCHER R. H.: *Computational Fluid Mechanics and Heat Transfer.* Taylor & Francis, Washington 1997.

[10] MARTYNENKO O.G., SOKOWISKYN J.A.: *Natural Convection Heat Transfer on the Vertical Surface.* Nauka, Minsk 1977 (in Russian).